Rediscovering our Galaxy
Proceedings IAU Symposium No. 334, 2017
C. Chiappini, I. Minchev, E. Starkenburg
& M. Valentini, eds.

doi:10.1017/S1743921317006573

NIHAO-UHD: High-resolution Simulations of MW mass galaxies

Tobias Buck[1], Andrea Macciò[2], Melissa Ness[1], Aura Obreja[3] and Aaron Dutton[2]

[1]Max-Planck Institut für Astronomie, Königstuhl 17, D-69117 Heidelberg, Germany
[2]New York University Abu Dhabi, PO Box 129188, Abu Dhabi, UAE
[3]Universitäts-Sternwarte München, Scheinerstrae 1, D-81679 München, Germany

Abstract. High resolution cosmological and hydrodynamical simulations have reached a resolution able to resolve in a self consistent way the disc of our galaxy, the galaxy center and the satellites orbiting around it. We present first results from the NIHAO-UHD project, a set of very high-resolution baryonic zoom-in simulations of Milky Way mass disc galaxies. These simulations model the full cosmological assembly history of the galaxies and their satellite system using the same, well tested physics as the NIHAO project. We show that these simulations can self-consistently reproduce the observed kinematical and morphological features of the X-shaped bulge observed in our own Milky Way.

Keywords. Galaxy: bulge – Galaxy: evolution – Galaxy: formation – Galaxy: kinematics and dynamics – Galaxy: structure – Galaxy: center – methods: numerical

1. Introduction

The very center of our own Galaxy shows a complex morphology and it is long known that it hosts a boxy/peanut shaped bulge and a galactic bar (e.g. Okunda *et al.* 1977). The major axis of the Galactic bar is about 27° inclined with respect to the line of sight (los) and it reaches out to about 3.5 kpc (Gerhard 2002). The red clump stars in the center of our Galaxy are split into two components well separated along the los (Ness *et al.* 2013a) with the interpretation of an underlying X-shaped structure in the bulge (McWilliam & Zoccali 2010, Nataf 2010) which further shows different properties for different metallicity sub-populations (Rojas-Arriagada *et al.* 2014). The formation scenario of boxy/peanut-shaped bulges is well studied in isolated N-body simulations which show that these bulges can form in-situ via disc instabilities (Athanassoula & Martinez-Valpuesta 2009) where flat discs develop a bar which then puffs up into a boxy/peanut bulge structure via a vertical instability (Bureau & Athanassoula 2005; Debattista *et al.* 2006). However, there is no agreement as to what orbits actually make up the boxy/peanut bulge of our Galaxy (see e.g. Portail *et al.* 2015b,a). New large scale galactic surveys as e.g. the BRAVA (Howard *et al.* 2008), ARGOS (Freeman *et al.* 2013) and APOGEE surveys (Majewski *et al.* 2015) delivered new high quality data of large samples of stars in the Galactic bulge. In order to interpret the new data we need improved models and high-resolution simulations. E.g., Debattista *et al.* (2017) compared idealized high-resolution N-body simulations to the Milky Way (MW) data from APOGEE and found that initially co-spatial populations of stars can be separated by a bar. Athanassoula *et al.* (2017) on the other hand are able to reproduce the observed signatures of the MW bulge with isolated hydrodynamical simulations of wet galaxy mergers. Due to their idealized setup, these simulations achieve very high spatial resolution but not a realistic environment nor cosmological growth history of the galaxy. Here we use, for the first time, a fully cosmological simulation of galaxy formation to study the inner region of a galaxy showing a bulge that is very similar to that of the MW.

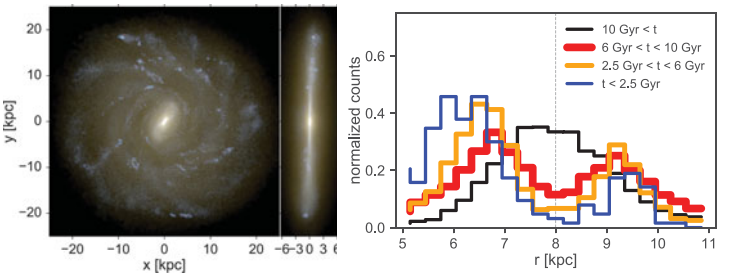

Figure 1. *Left panel*: Stellar composite image of the galaxy in face-on and edge-on projections. i, v, u-band fluxes are used to create the r,g,b maps. *Right panel*: Star counts as a function of distance from the sun in different age bins for loss going through the center of the galaxy ($-2.0° < l < 2.0°$) at a height of $6.5° < |b| < 10°$ above the galactic plane.

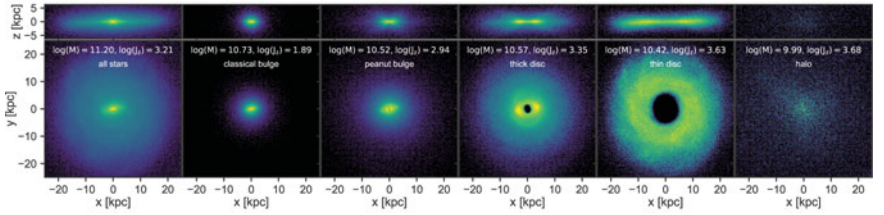

Figure 2. Surface density plots of kinematically decomposed populations of stars in our simulation. Each panel indicates the total mass in solar masses and the total specific angular momentum in each component.

2. The Simulation

The simulation analyzed in this work is a higher-resolution version of the galaxy g2.79e12 from the NIHAO sample (Wang *et al.* 2015). The hydrodynamics, star formation recipes and feedback schemes exploited are the same as for the original NIHAO runs. Galaxies from the NIHAO sample have been proven to match remarkably well many observed properties of galaxies (Gutcke *et al.* 2016; Dutton *et al.* 2017; Buck *et al.* 2017).

This galaxy has been run using cosmological parameters from the Planck Collaboration *et al.* (2014) and the mass resolution is $m_{\rm dark} = 5.141 \times 10^5 {\rm M}_\odot$, $m_{\rm gas} = 9.382 \times 10^4 {\rm M}_\odot$, $m_{\rm star} = 1/3 \times m_{\rm gas} = 3.127 \times 10^4 {\rm M}_\odot$. The corresponding force softenings are $\epsilon_{\rm dark} = 620$ pc and $\epsilon_{\rm gas} = \epsilon_{\rm star} = 265$ pc. The final total mass within the virial radius ($\rm R_{vir} \sim 300$ kpc) is $\rm M_{tot}$=$3.13 \times 12 {\rm M}_\odot$, the dark matter mass is $\rm M_{dark}$=$2.78 \times 12 {\rm M}_\odot$, the stellar mass is $\rm M_{star}$=$1.42 \times 11 {\rm M}_\odot$ and the gas mass is $\rm M_{gas}$=$4.93 \times 10 {\rm M}_\odot$. The galaxy's stellar disk has a scale length of $\rm R_d \sim 5$ kpc and a scale height of $\rm H_z \sim 500$ pc within the innermost 5 kpc. An impression of the galaxy's face-on and edge-on projections is given in the left panel of Fig. 1. The pronounced bar of this simulation is clearly visible. In the analysis that follows we place the Sun at (x,y,z)=(8,0,0) kpc and rotate the simulation such that the bar is inclined at 27° with respect to the los to match the position of the Sun in the MW (Wegg & Gerhard 2013). In the right panel of Fig. 1 we show the los number counts of stellar particles through the center of the simulated galaxy ($l = 0°$, $6.5° < |b| < 10°$), We split the stellar populations into several age bins. Up to the oldest stars of 10 Gyr we see a double peaked distribution which is indicative of the X-shaped morphology of the bulge. The two peaks are the result of the los cutting to the near arm of the X (peak at $\sim 6-7$ kpc) in front of the galactic center and through the far arm behind the galactic center (peak at $\sim 9-10$ kpc) and in excellent agreement with the observation from the ARGOS survey (see Ness *et al.* 2013a).

https://doi.org/10.1017/S1743921317006573 Published online by Cambridge University Press

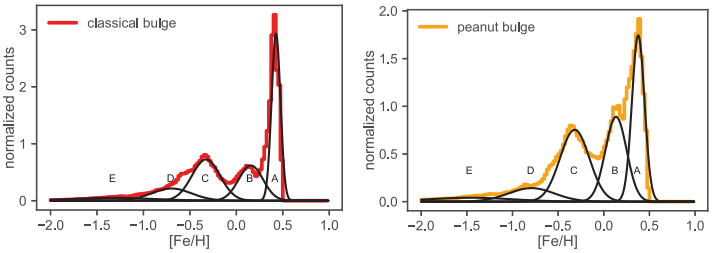

Figure 3. Chemical sub-components of the kinematically decomposed spherical/classical bulge (left panel) and the peanut bulge (right panel). Similar to the MW we identify 5 different sub-components A to E.

3. The Bulge region

In order to study the bulge region of the simulation we use the method presented in Obreja *et al.* (2016) to decompose the stellar particles of the simulation into kinematically different sub-populations. We identify 5 different sub-populations by separating stars on different orbit distributions into different populations. In Fig. 2 we show the surface density plots in edge-on and face-on projections of all five sub-components. Although separating the stellar particles solely based on their kinematics we find the sub-populations to also separate in their morphologies. For the remainder of this paper we focus on the two bulge components.

3.1. *Metallicity distribution of bulge stars*

Having kinematically identified the stellar particles which belong to the bulge of the galaxy we study the metallicity distribution of the two bulge components in Fig. 3. Both bulge components show very similar metallicity distributions with a large spread in [Fe/H] from ~ -1.5 to ~ 0.5. In both components we identify 5 different metallicity peaks well in agreement with the observations of the ARGOS survey (Ness *et al.* 2013b) and the microlensed dwarf sample of Bensby *et al.* (2017a). The occurrence of different metallicity sub-components is indicative of different populations contributing to the bulge. Metal rich stellar particles are coming from the thin disc and stellar particles of intermediate metallicity are coming from a thick disc component. Metal poor stars on the other hand belong to an old merger generated population. Thus, we find in agreement with previous studies for the MW that the bulge region is not a unique stellar population, but rather the central region where all the other Galactic populations widely overlap Bensby *et al.* (2017b).

3.2. *Kinematics of the bulge stars*

Although on different orbital families the stellar populations of the two bulge components show very similar properties. For the following analysis we look at the kinematics of the stellar particles in both bulge components together. We split the stellar particles into the five metallicity components identified in Fig. 3 and look at their kinematics. For the MW, the ARGOSS survey provides kinematics of the stars in different metallicity populations very similar to the simulation (Ness *et al.* 2013b). In Fig. 4 we compare the rotation (mean los velocity, upper panels) and dispersion profile (los velocity dispersion, lower panels) in galactic coordinates of both the simulation and the observation. Simulated data is shown in colored dots/triangles and observations are shown in colored bands (full sample, left most panels) and gray bands (metallicity sub-components). We find that the simulation can well reproduce the observed rotation and dispersion profiles for the whole sample (left panel). The rotation and dispersion profiles of components A, B and C are well in agreement with what is observed for the MW. We find a cylindrical

https://doi.org/10.1017/S1743921317006573 Published online by Cambridge University Press

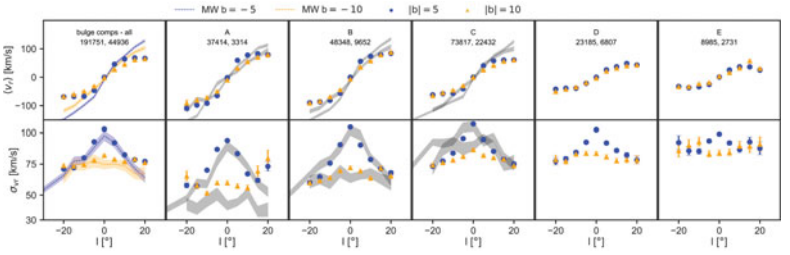

Figure 4. Rotation (upper panels) and dispersion profiles (lower panels) for stellar particles both from the spherical/classical bulge and the peanut bulge in different metallicity sub-components. Measurements from ARGOS are shown with colored lines (whole sample) and gray bands (sub-populations). Colored dots/triangles show the result obtained for our simulation.

rotation profile and a triangular shaped dispersion profile close to the disc ($b = -5°$) and a flat dispersion profile far from the disc ($b = -10°$). In particular, we find excellent agreement for the dispersion profile of population B. For the components D and E we find that the simulation can well reproduce the almost latitude independent dispersion seen for stars –0.5 > [Fe/H] > –1.0 and the very hot population with a large scatter in the measured dispersion for stars [Fe/H] < –1.0 measured in the ARGOS survey (not shown here, but see Ness *et al.* 2013b). Especially, we find that observed profiles can not simply be explained by a peanut bulge alone but need in addition a classical bulge component which is in agreement with recent results from Debattista *et al.* (2016). Thus, we predict that if with future surveys we are able to get orbital information for stars in the bulge we would be able to disentangle different kinematical components of the bulge.

References

E. Athanassoula & I. Martinez-Valpuesta. *ASSP*, 8:77, 2009.
E. Athanassoula, S. A. Rodionov, & N. Prantzos. *MNRAS*, 467:L46–L50, May 2017.
T. Bensby, S. Feltzing, A. Gould, *et al. ArXiv e-prints*, July 2017.
T. Bensby, S. Feltzing, A. Gould, *et al. ArXiv e-prints*, February 2017.
Buck, T., Macciò, A. V., Obreja, A., *et al. MNRAS*, 468, 3628, July 2017
M. Bureau & E. Athanassoula. *ApJ*, 626:159–173, June 2005.
V. P. Debattista, L. Mayer, C. M. Carollo, *et al. ApJ*, 645:209–227, July 2006.
V. P. Debattista, M. Ness, O. A. Gonzalez, *et al. MNRAS*, 469, 1587, August 2017.
A. A. Dutton, A. Obreja, L. Wang, *et al. MNRAS*, 467, 4937, June 2017
K. Freeman, M. Ness, E. Wylie-de-Boer, *et al. MNRAS*, 428:3660–3670, February 2013.
O. Gerhard. *Astronomical Society of the Pacific Conference Series*, page 73, 2002.
T. A. Gutcke, G. S. Stinson, A. V. Macciò, *et al. MNRAS*, October 2016.
C. D. Howard, R. M. Rich, D. B. Reitzel, *et al. ApJ*, 688:1060–1077, December 2008.
S. R. Majewski, R. P. Schiavon, P. M. Frinchaboy, *et al. ArXiv e-prints*, September 2015.
A. McWilliam & M. Zoccali. *ApJ*, 724:1491–1502, December 2010.
D. M. Nataf, A. Udalski, A. Gould, *et al. ApJ*, 721, L28, September 2010.
M. Ness, K. Freeman, E. Athanassoula, *et al. MNRAS*, 430:836–857, April 2013.
M. Ness, K. Freeman, E. Athanassoula, *et al. MNRAS*, 432:2092–2103, July 2013.
A. Obreja, G. S. Stinson, A. A. Dutton, *et al. MNRAS*, 459:467–486, June 2016.
H. Okuda, T. Maihara, N. Oda, *et al. Nature*, 265:515, February 1977.
Planck Collaboration *A&A*, 571:A16, November 2014.
M. Portail, C. Wegg, & O. Gerhard. *MNRAS*, 450:L66–L70, June 2015.
M. Portail, C. Wegg, O. Gerhard, *et al. MNRAS*, 448:713–731, March 2015.
A. Rojas-Arriagada, A. Recio-Blanco, V. Hill, *et al. A&A*, 569:A103, September 2014.
L. Wang, A. A. Dutton, G. S. Stinson, *et al. MNRAS*, 454:83–94, November 2015.
C. Wegg & O. Gerhard. *MNRAS*, 435:1874–1887, November 2013.

https://doi.org/10.1017/S1743921317006573 Published online by Cambridge University Press